

High-resolution beam steering using microlens arrays

Ata Akatay, Caglar Ataman, and Hakan Urey

Department of Electrical Engineering, Koc University, Sariyer, Istanbul 34450, Turkey

Received June 1, 2006; accepted July 5, 2006;

posted July 17, 2006 (Doc. ID 71583); published September 11, 2006

Imaging or beam-steering systems employing a periodic array of microlenses or micromirrors suffer from diffraction problems resulting from the destructive interference of the beam segments produced by the array. Simple formulas are derived for beam steering with segmented apertures that do not suffer from diffraction problems because of the introduction of a moving linear phase shifter such as a prescan lens before the periodic structure. The technique substantially increases the resolution of imaging systems that employ microlens arrays or micromirror arrays. Theoretical, numerical, and experimental results demonstrating the high-resolution imaging concept using microlens arrays are presented. © 2006 Optical Society of America
OCIS codes: 050.1940, 050.5080, 120.5800, 170.3890, 350.3950.

Mirror-based systems are commonly used for scanning and beam-steering applications but require beam folding due to the reflective mirror.¹ Refractive elements such as microlens arrays (MLAs) can be used in beam scanning^{2,3} as well as in beam expansion⁴ and light-homogenization applications.⁵ Beam scanning can be achieved by lateral translation of two single lenses separated by two focal lengths. Beam scanning with refractive lenses does not require beam folding, and such a system can fit into a small cross-sectional area.⁶ Beam scanning by two MLAs separated by two focal lengths offers further advantages such as large scan angles obtained at smaller deflections (i.e., half the diameter of a microlens) and better aberration performance because of the smaller lenses. The main disadvantage of the scheme is that only discrete diffraction angles can be addressed because of the periodic nature of the MLA.² Once the diffraction problem is solved, a beam-scanning MLA system would be favorable especially in applications requiring a compact scanning system or scanning of a large beam.

In this Letter, we present, for what is believed to be the first time, a solution to the diffraction-related discrete addressing problem while maintaining all the advantages of high-resolution scanning with MLAs. The solution presented here can be applied for beam steering with micromirror array devices as well.⁷

Figure 1 illustrates the three-MLA beam-steering system, including a movable prescan lens (PSL), a movable MLA (MMLA), and two MLAs (DMLA) separated by one focal length that are joined together (either on the same substrate or from two separate pieces),⁴ followed by an imaging lens for focusing. All three MLAs in the train have unit diameter d and focal length f_{MLA} and are separated by f_{MLA} . The lateral displacements of the PSL and the MMLA are r_1 , r_2 , respectively. When the MMLA is moved, the middle MLA acts as a field lens and eliminates interchannel cross talk between MLA channels and spurious light at the last MLA surface.⁸

One major problem with the MLA scanning system is discrete angular addressability due to the periodic nature of the MLA. A novel solution to the problem is

tilting the beam before the MMLA by moving the PSL. Figure 2 illustrates the physical optics view and the operation of the system. Two parameters of interest are illustrated after each element in the system: beam tilt angle θ and the optical path length difference (OPD) between the neighboring channels (i.e., the segments of the wavefront). The lateral displacements of the PSL and the MMLA result in independent contributions to the beam scan angle:

$$\alpha = -r_1/f_{PSL}, \quad \beta = r_2/f_{MLA}. \quad (1)$$

The total scan angle $\alpha + \beta$ can be calculated using superposition. To analyze the PSL's contribution to the beam scan angle, the three-MLA block can be modeled as a parallel channelized processor, where each channel consists of three identical lenses with one focal distance separation and analyzed using Fourier optics. Figure 3(a) illustrates the propagation of a

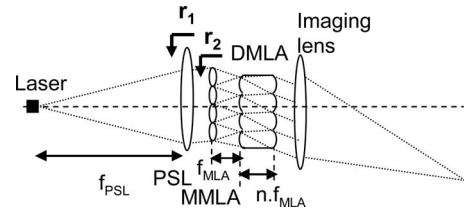


Fig. 1. Ray-tracing view of the microlens beam steering system. r_1 and r_2 are the displacements of the PSL and the MMLA.

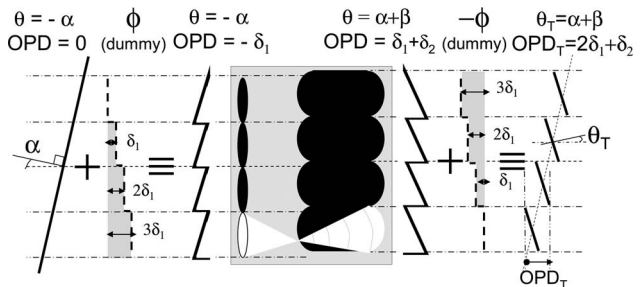


Fig. 2. Physical optics view of the three-MLA block system after the PSL. Scan angle and OPD between beam segments is marked after each element. (Dummy phase shifters have no net effect in the system.)

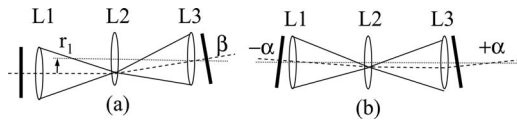


Fig. 3. Propagation of a collimated beam through a three-microlens channel when (a) L1 is displaced by r_1 and (b) the incident beam is tilted with angle α .

plane wave through a three-lens system when the coordinate axis of lens 1 is shifted. Lens L1 forms a focused spot, and the L2 and L3 combination forms an optical Fourier transform module and converts the displaced spherical wavefront into a plane wave with tilt angle β (Chap. 4 of Ref. 9). Figure 3(b) illustrates that if a tilted plane wave of angle $(-\alpha)$ were incident on three identical lenses on the same optical axis, the propagation vector would become parallel to the optical axis after L2; therefore, the exiting wavefront would be another plane wave with angle $(+\alpha)$, which is effectively rotated by 2α .

For the purpose of Fourier analysis, the incident planar wavefronts on each microlens channel can be made identical by adding a different linear phase at the entrance of each channel, which is then subtracted at the exit of each channel; thus the net effect of the phase shifters is zero. As illustrated in Fig. 2, the dummy phase function forms a step function (ϕ) with step heights of $\delta_1 = ad$, which corresponds to the OPD between neighboring channels. Thus, the contributions of the PSL to θ and the OPD can be calculated as α and $2\delta_1$, respectively. In the same manner, assuming a plane parallel wave incident on the three-MLA block, the MMLA contributions to θ and the OPD can be calculated as β and $\delta_2 = \beta d$, respectively. The total beam scan angle θ_T and the phase difference between wavefront segments at the exit of the system, OPD_T , are expressed as the sum of independent contributions of the PSL and the MMLA:

$$\theta_T = \alpha + \beta, \quad (2)$$

$$OPD_T = 2\delta_1 + \delta_2 = (2\alpha + \beta)d. \quad (3)$$

Constructive interference between wavefront segments is required to achieve the smallest point spread function (PSF) for the focused spot. Therefore, the OPD_T in Eq. (3) should satisfy the following phase condition for all α and β :

$$OPD \equiv n\lambda, \quad n = 0, \pm 1, \pm 2, \dots \quad (4)$$

Therefore, arbitrary scan angles θ_T can be achieved by choosing r_1 and r_2 subject to the above condition as follows:

$$r_1 = (\theta_T - n\lambda/d)f_{\text{PSL}}, \quad r_2 = (\theta_T + r_1/f_{\text{PSL}})f_{\text{MLA}}. \quad (5)$$

Figure 4 is the simulated PSF of the system in normalized angular coordinate system assuming plane-wave illumination, a square-packed 100% fill-factor spherical MLA, and a thin lens approximation. A combination of angular and far-field beam propagation methods were employed (Chaps. 3 and 4 of Ref. 9). In Figs. 4(a) and 4(c), the PSL remains centered, and the diffraction angles due to the periodic nature

of the MLA at $\pm n\lambda/d$ (n integer) can be addressed by the MMLA motion only. For Fig. 4(b), $\theta_T = 0.25\lambda/d$ and $OPD = 0.25\lambda$, therefore, the phase condition is not met and the resultant PSF is split between two diffraction orders. Figure 4(d) shows that, when α and β are properly selected to meet the phase condition, a constructive PSF at $\theta_T = 0.25\lambda/d$ is obtained.

For the experimental demonstration, a full system similar to that in Fig. 1 was built with both the PSL and the MMLA mounted on moving stages. The $f/5$ MLAs have a nearly 100% fill factor and $200\ \mu\text{m}$ pitch size. Figure 5 illustrates how the PSF changes with PSL and MMLA motion and the phase condition. As was illustrated in Figs. 4(b) and 4(d), the scan angles that are not addressable by the MMLA motion alone can be addressed with the combined motion of the MMLA and the PSL. Experimental results show that the PSL's motion moves both the entire diffraction grid and the centroid of the PSF by the same amount but in opposite directions, which can be verified using Eqs. (3) and (4). The MMLA motion, however, moves only the centroid of the intensity pattern, while the diffraction grid stays stationary.

Figure 6(a) demonstrates the discrete addressing problem in beam steering using microlens arrays, and Fig. 6(b) demonstrates that continuous address-

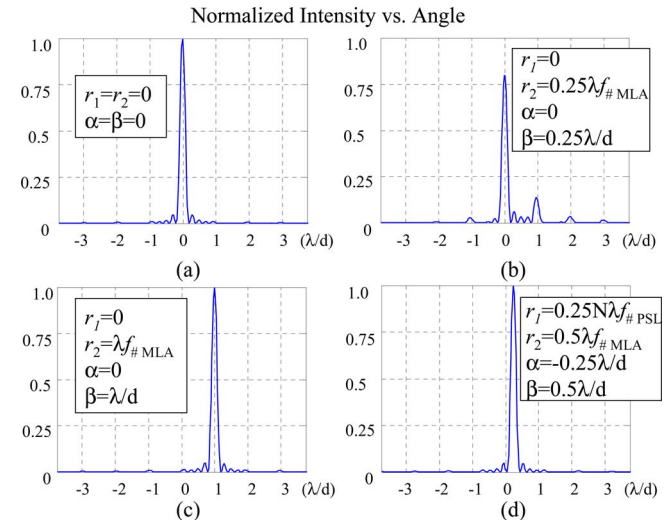


Fig. 4. (Color online) Simulated PSF for different amounts of the PSL and the MMLA displacements (r_1 and r_2) and the resultant beam tilt angles α and β . (a), (c), and (d) illustrate constructive beam interference (phase condition is met), and (b) illustrates destructive interference (phase condition is not met).

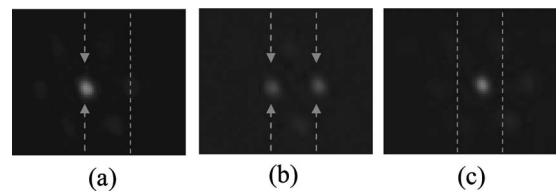


Fig. 5. Experimental results for the MMLA and the PSL's motion: (a) all lenses on axis, (b) only the MMLA is moved to steer beam by half-diffraction angle (phase condition not met); (c) both the PSL and the MMLA are moved to steer the beam by half-diffraction angle (phase condition met).

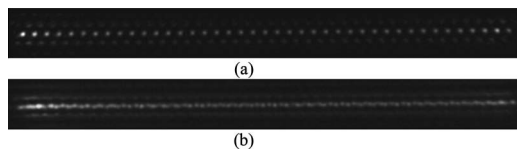


Fig. 6. Experimental results of the line scans: (a) MMLA motion produces only discrete addressing, (b) PSL and the MMLA move synchronously and the phase condition is met at all times and continuous addressing is achieved (imperfections in the line are due to slight misalignment of the setup).

Table 1. System Features and Resolution^a

| D (mm) | $f_{\#,\text{MLA}}$ | d (mm) | # of μ lenses | $r_{1,\text{max}}$ (μm) | θ_{max} (mrad) | N_R |
|-------------|---------------------|-------------|----------------------|---|---------------------------------|-------|
| 1.5 | 4 | 0.1 | 12 | ± 14 | ± 125 | 576 |
| 1.5 | 4 | 0.2 | 7.5 | ± 7 | ± 125 | 576 |
| 3 | 4 | 0.2 | 30 | ± 28 | ± 125 | 1152 |
| 3 | 4 | 0.2 | 15 | ± 14 | ± 125 | 1152 |
| 3 | 3 | 0.1 | 30 | ± 28 | ± 167 | 1536 |
| 3 | 2 | 0.1 | 30 | ± 28 | ± 250 | 2304 |

^aUniform laser illumination at $\lambda=632$ nm. Full width at half-maximum spot size is considered. $f_{\#,\text{PSL}}=3$.

ability is possible using combined synchronous motion of the PSL and the MMLA and proves our concept. A line scan with more than 200 resolvable spots has been demonstrated with the proposed method.

Neglecting the aberrations and assuming that the paraxial approximation is valid (i.e., small angles), the number of resolvable spots (N_R) that can be obtained by this scanning system can be expressed as¹⁰

$$N_R = \frac{2\theta_{\text{max}}D}{K\lambda} = \frac{D}{Kf_{\#,\text{MLA}}\lambda}, \quad (6)$$

where θ_{max} is the maximum optical scan angle and K is a beam constant that incorporates the beam profile and Gaussian beam-clipping effects and the assumptions related to the system design such as amount of overlap between adjacent pixels.

Table 1 shows the system resolution as a function of system parameters assuming diffraction-limited performance. Maximum resolution of 2300 pixels in each axis can be achieved with a 3 mm clear aperture and $f/2$ microlenses using the assumptions and the formulas in Refs. 1 and 10. A scan angle of ± 0.25 rad can be achieved by moving the PSL and the MMLA by ± 28 μm and ± 50 μm , respectively. To achieve the same scan angle and resolution with a 3 mm clear aperture, an $f/2$ lens beam-steering system would need to move by ± 1500 μm , and a scanning mirror would have a total tip deflection of ± 189 μm . For the fastest system operation, the PSL should operate in resonant mode and the MMLA should operate in nonresonant mode (the details of the actuation and waveforms will be discussed in a future publication).

Assuming the PSL moves at 25 kHz, depending on the other system parameters, data rates in the range 0.5–2 Mpixel/s can be obtained. Alternatively, the MMLA can be operated in resonant mode by using a fast-switching nonmechanical beam steerer, e.g., acousto-optic deflectors or spatial light modulators, in place of the PSL. In such a configuration, data rates higher than 10 Mpixels/s are achievable.

In summary, we have formulated and demonstrated a simple solution to the discrete addressing problem encountered in beam-steering systems that use microlens arrays and micromirror arrays. The solution presented eliminates a serious limitation of such systems and can be applied anytime a periodic structure with tilted wavefront incidence is encountered. The system demonstrated in this work uses a PSL that moves together with the MMLA subject to a phase condition given in Eq. (3) and achieved 200 pixel continuous addressability using 1 mm clear aperture, 200 μm diameter, $f/5$ microlenses mounted on simple CD actuators. The proposed laser-scanning system can be used for high-resolution and high-speed 2D imaging applications using two moving components mounted on xy stages.

Compared with other laser-beam-scanning methods, MLA-based scanning system requires smaller mechanical deflections and all components can be placed in line for a more compact and faster system incorporating compact micro xy stages, such as those produced with microelectromechanical-system technology. Such in-line imaging systems have advantages in applications such as endoscopic instruments and scanning laser vibrometers. In addition, the scheme is suitable for region-of-interest type image capture operation modes. The system operation is wavelength dependent and is suitable for narrow-band illumination. Multicolor operation is possible by employing different color sources time sequentially (the data rate reduces to 1/3). Likewise, imaging with different excitation and fluorescence wavelengths is possible using additional light detectors.

A. Akatay's e-mail address is aakatay@ku.edu.tr.

References

1. H. Urey, in *Encyclopedia of Optical Engineering*, R. G. Driggers, ed. (Marcel Dekker, 2003), pp. 2445–2457.
2. E. A. Watson, *Opt. Eng.* **32**, 2665 (1993).
3. J. Duparre and R. Göring, *Appl. Opt.* **42**, 3992 (2003).
4. H. Urey and K. Powell, *Appl. Opt.* **44**, 4930 (2005).
5. F. Nikolajeff, S. Haard, and B. Curtis, *Appl. Opt.* **36**, 8481 (1997).
6. H. Miyajima, K. Murakami, and M. Katashiro, *IEEE J. Sel. Top. Quantum Electron.* **10**, 514 (2004).
7. E. A. Watson and A. Miller, in *Proc. SPIE* **2687**, 60 (1996).
8. J. Duparre, D. Radtke, and P. Dannberg, *Appl. Opt.* **43**, 4854 (2004).
9. J. W. Goodman, *Introduction to Fourier Optics* (McGraw-Hill, 1996).
10. H. Urey, *Appl. Opt.* **43**, 620 (2004).